ARMA 21–1250

The Influence of Heterogeneity of Block Contact Input Parameters on Model Behavior for Bonded Block Models of Laboratory Rock Specimens

West, I.
Colorado School of Mines, Golden, CO, USA
Walton, G.
Colorado School of Mines, Golden, CO, USA

This paper was prepared for presentation at the 55th US Rock Mechanics/Geomechanics Symposium held in Houston, Texas, USA, 20-23 June 2021. This paper was selected for presentation at the symposium by an ARMA Technical Program Committee based on a technical and critical review of the paper by a minimum of two technical reviewers. The material, as presented, does not necessarily reflect any position of ARMA, its officers, or members. Electronic reproduction, distribution, or storage of any part of this paper for commercial purposes without the written consent of ARMA is prohibited. Permission to reproduce in print is restricted to an abstract of not more than 200 words; illustrations may not be copied. The abstract must contain conspicuous acknowledgement of where and by whom the paper was presented.

ABSTRACT: Bonded Block Models (BBMs) have become increasingly used to simulate laboratory rock samples in Unconfined Compressive Strength (UCS) and Triaxial tests. BBMs require input parameters that describe the deformation of the blocks themselves (block properties), as well as the interaction of the blocks with adjacent blocks (contact properties). For rocks with more than one mineral (i.e. block) type, there exists more than one type of contact between blocks, each of which requires a different set of input parameters. Little is known about the effect of heterogeneity of the contact properties on individual aspects of the overall behavior of the BBM. Therefore, this study has conducted a sensitivity analysis on the heterogeneity of contact input parameters. Contact input parameters were tested separately by varying the degree of heterogeneity between contact types, while keeping the weighted average of each given contact property constant for all simulations. Both a UCS and a Triaxial test with 12 MPa of confining pressure were simulated for each case to evaluate the effects of heterogeneity under unconfined and confined conditions. Rock specimen properties were computed from the model results including Young's Modulus, Poisson's Ratio, UCS and Peak Strengths, and Crack Initiation (CI) and Crack Damage (CD) parameters. While several minor influences of heterogeneity on macroscopic properties were noted, the primary influence was that of contact peak cohesion heterogeneity on CD under both unconfined and confined conditions.

1. INTRODUCTION

With the advent of high-performance computing, numerical models have become increasingly used to study rock behavior. Numerical models can be used to complement laboratory testing, as they require significantly less time and labor to complete. Unconfined Compressive Strength (UCS) and Triaxial tests are laboratory tests that are commonly used to assess the material properties of intact rock. Such laboratory tests can be simulated using Bonded Block Models (BBMs) (Sinha and Walton, 2020) and can be further applied to field-scale modeling scenarios like excavations, roof stability, underground pillar design, and other scenarios that cannot be tested in a laboratory.

BBMs are a subset of discrete element method (DEM) modeling where material is broken into continuous elements that interact discretely with adjacent elements. The deformations of the continuous elements, as well as their interaction with adjacent elements, are governed by a series of input parameters (Jing, 2003). Each input parameter affects the model's macroscopic behavior uniquely, and many studies have previously analyzed the effect that the variation of these input parameters has on the macroscopic behavior of the model (Ghazvinian et al, 2014; Cai and Noorani, 2015; Bahaaddini and Rahimi, 2018; Wang and Cai, 2019).

Specifically, BBMs use polygonal blocks as the continuous elements, which can be modeled as rigid, elastic, or inelastic (Ghazvinian et al., 2014). Elastic blocks have been the most commonly used, but inelastic blocks have been found to more accurately replicate the behavior of intact rock, particularly in the post-peak regime and under higher confinements (Sinha and Walton, 2020). BBMs are attractive for modeling intact rock because the polygonal blocks can be generated with specified sizes and shapes. And therefore, the geometry of the blocks can be set to approximate the shape of the mineral grains in real rock. Furthermore, the interaction of the blocks with adjacent ones is analogous to the interaction between mineral grains within real rock. Contacts within DEMs can break, simulating the loss of cohesion that occurs at grain-to-grain contacts in rock as damage accumulates. For these reasons, BBMs have been increasingly used to model rock (Norouzi et al., 2013).

For rocks with more than one mineral (i.e. block) type, there exists more than one type of contact between blocks, each of which requires a different set of input parameters (Chen et al., 2016). Previous studies have found that this heterogeneity of block contact properties can be used to help match all attributes of rock behavior (Sinha and Walton, 2020), but little is known about the effect of heterogeneity of the contact properties on individual aspects of the overall mechanical behavior of the BBM. Elastic block property inputs are density, Young's Modulus, and Poisson's Ratio, which can be easily constrained in the laboratory (Bass, 1995). On the other hand, contact properties cannot be measured in the laboratory and must be back-calculated via a calibration process. This calibration process entails varying contact input parameters until the macroscopic behavior of the BBM matches laboratory data (Wang and Cai, 2019). The more contact types that exist in a BBM, the more unique inputs the model requires for calibration. Different values for the same input parameter can be used for each contact type. This variation in values within one input parameter affects the model's behavior (Chen and Konietzky, 2014).

With all this in mind, this paper documents a sensitivity analysis on the heterogeneity of contact input parameters within an elastic BBM. A BBM with elastic blocks was used rather than one with inelastic blocks due to its model run-time considerations and because elastic BBMs are more widely used (Sinha and Walton, 2020). The contact parameters considered in the study were normal and shear stiffnesses, peak cohesion, peak friction angle, peak tensile strength, residual friction angle, and dilation angle. Although BBMs require residual cohesion and residual tensile strength inputs as well, these were not considered, as they are zero for brittle rock (Stavrou and Murphy, 2018). Trends in macroscopic material properties like Young's Modulus, Poisson's Ratio, UCS and peak strengths, and Crack Initiation (CI) and Crack Damage (CD) parameters as a function of contact property heterogeneity were analyzed for each model.

2. MODEL SET UP

A previously developed elastic BBM of Blanco Mera granite (West et al., 2020) that was calibrated to laboratory data (Alejano et al., 2017; Walton et al., 2018) was used for this study. Blanco Mera granite contains four different major mineral types (plagioclase, quartz, alkali feldspar, and mica) and therefore contains 10 distinct contact types. A description of the real rock, BBM block generation, and mineral grain assignment for the BBM is provided by West et al., 2020. Additionally, discussion on the assignment of block density and elastic parameter values is included. A modified calibration from that of West et al., 2020 was used as the starting point for the current study. These base input parameter values are listed in Table 1.

These base contact input parameter values were systematically varied, corresponding to an increase or decrease in heterogeneity across contact types. The goal of this sensitivity analysis was to isolate the influence of input parameter heterogeneity, while keeping the mean value of each property constant for all simulations. Therefore, a heterogeneity factor was created to quantify the degree of parameter heterogeneity relative to the base parameter set and the weighted average input value. This heterogeneity factor (HF) is calculated via Eq. (1):

$$HF = \frac{Value_f - WA}{Value_0 - WA} \quad (1)$$

Table 1. Micro-parameters of the base BBM from West et al., 2020 with a modified calibration to laboratory data (Alejano et al., 2017; Walton et al., 2018). Definitions of parameter abbreviations are: k_n = joint normal stiffness, k_s = joint shear stiffness, c = cohesion, ϕ = friction angle, jt = tensile strength, c_{res} = residual cohesion, jt_{res} = residual tensile strength, Ψ = dilation angle.

Property /*Contact*	**k_n (GPa/m)**	**k_s (GPa/m)**	**c (MPa)**	**Φ (°)**	**jt (MPa)**	**c_{res} (MPa)**	**Φ_{res} (°)**	**jt_{res} (MPa)**	**Ψ (°)**
Mica-Mica	3.3E+04	1.3E+04	46.6	56.5	29.5	0	3.0	0	5.0
Quartz-Quartz	7.1E+04	2.8E+04	75.8	63.5	40.8	0	3.0	0	5.0
Plagioclase-Plagioclase	6.3E+04	2.5E+04	65.3	61.5	43.2	0	3.0	0	5.0
Feldspar-Feldspar	5.8E+04	2.3E+04	64.2	61.5	40.8	0	3.0	0	5.0
Quartz-Plagioclase	5.8E+04	2.3E+04	52.4	58.5	24.6	0	3.0	0	5.0
Quartz-Mica	5.8E+04	2.3E+04	46.6	53.5	93.4	0	3.0	0	5.0
Plagioclase-Mica	5.8E+04	2.3E+04	31.5	53.5	26.2	0	3.0	0	5.0
Plagioclase-Feldspar	5.3E+04	2.1E+04	63.0	58.5	37.4	0	3.0	0	5.0
Feldspar-Mica	5.8E+04	2.3E+04	35.0	53.5	13.3	0	3.0	0	5.0
Feldspar-Quartz	6.8E+04	2.7E+04	44.3	58.5	33.0	0	3.0	0	5.0

where $Value_f$ is the new value for a given input parameter, $Value_0$ is the original value used in the base BBM (per Table 1), and WA is the weighted average of the contacts' values for a given input parameter. A heterogeneity factor greater than 1 indicates an increase in heterogeneity from the base and a factor less than 1 indicates a decrease in heterogeneity from the base.

The weighted average is calculated by multiplying each of the base contact property values by their respective proportions, and then summing these numbers. Table 2 shows the percentages of the ten contact types within the Blanco Mera granite BBM.

Table 2. Percentages of contact types within the Blanco Mera granite BBM (West et al, 2020).

Contact Type	Percentage
Mica-Mica	4.80%
Quartz-Quartz	2.28%
Plagioclase-Plagioclase	9.12%
Feldspar-Feldspar	8.64%
Quartz-Plagioclase	12.41%
Mica-Quartz	7.57%
Mica-Plagioclase	12.51%
Feldspar-Plagioclase	19.98%
Mica-Feldspar	13.04%
Feldspar-Quartz	9.65%
TOTAL	100.00%

Eq. (1) can be rearranged to calculate a new value ($Value_f$) for each contact's input parameter, based on the original parameter from the base case (listed in Table 1), a specified heterogeneity factor (HF), and the weighted average of the contact values. This rearranged equation is included as Eq. (2):

$$Value_f = WA + HF * (Value_0 - WA) \qquad (2)$$

Simulations of UCS and Triaxial tests were run on the Blanco Mera BBM by varying the values of a single input parameter. All other input parameters were held constant per Table 1. These varied values were calculated using Eq. (2) with specified heterogeneity factors.

Eight heterogeneity factors were tested for joint normal stiffness, joint shear stiffness, peak cohesion, peak friction angle, and peak tensile strength input parameters. The ranges of the factors chosen were dictated by the constraint that none of the input parameters can be negative. The larger the heterogeneity factor, the more the input values deviate from their original value, so contacts with values less than the weighted average in the base case will become progressively smaller as the heterogeneity factor is increased. Eventually, with a very large HF, these contacts' input values will deviate so far from their original value that they become negative. Given this constraint, the eight heterogeneity factors used for joint normal stiffness, joint shear stiffness, peak cohesion, and peak friction angle are 2.00, 1.75, 1.50, 1.25, 1.00, 0.80, 0.67, 0.57, and 0.50. The eight heterogeneity factors used for peak tensile strength are 1.55, 1.40, 1.25, 1.10, 1.00, 0.91, 0.80, 0.71, and 0.65 (HFs for tensile strength are different from those of the other input parameters due to the constraint discussed previously). Note that the HF values that are less than 1 are equivalent to the reciprocals of the HF values greater than 1.

Residual friction angle and dilation angle are the remaining two input parameters tested in this study that have not yet been discussed. This is because the heterogeneity factor described in Eq. (1) does not apply for these parameters, since all contact types were assigned the same value in the base case (Table 1).

Therefore, a different approach was used that set minimum and maximum range values. These values became progressively spaced further apart from each other, corresponding to an increase in heterogeneity (see Tables 3 and 4). The ten contact types within the BBM were ranked on the basis of their peak cohesion (see Table 1), where the contact type with a rank of 1 was assigned the maximum value and the contact type with a rank of 10 was assigned the minimum value. Peak cohesion is the input parameter than predominantly affects the overall strength of a contact, so it was used to rank contacts on the basis of their strength. The eight contact types in between were assigned intermediate values between the maximum and minimum, following the order of rank, and maintaining the weighted average. The contact type rankings are also listed in Tables 3 and 4.

Each parameter set, corresponding to the HFs listed previously and to Tables 3 and 4, was assigned to the BBM, while all other input parameters were held constant (per Table 1). Two-dimensional UCS and Triaxial test simulations with 12 MPa of confining pressure were run for each of the parameter set variations. These two confinement levels are the bounds of the confinement range that the BBM was originally calibrated to (West et al., 2020).

Boundary conditions restricting movement in the vertical direction were applied to the bottom of the model, which represents the base platen used in real laboratory tests. A constant velocity boundary condition was applied to the top of the model, which simulates the lowering of the load frame on rock cores during UCS and Triaxial tests. The model was free to move in the lateral direction.

Table 3. List of input values for residual friction angle. Each column corresponds to a different set of parameters, where the "Range" (minimum value subtracted from maximum value) indicates the level of heterogeneity. 0 range is the base case listed in Table 1.

	Range	**0**	**1**	**2**	**3**	**4**	**5**
	Minimum	3.00	2.50	2.00	1.50	1.00	0.50
Ranking	Maximum	3.00	3.50	4.00	4.50	5.00	5.50
1	Quartz-Quartz	3.00	3.50	4.00	4.50	5.00	5.50
2	Plagioclase-Plagioclase	3.00	3.45	3.90	4.40	4.75	5.75
3	Feldspar-Feldspar	3.00	3.35	3.70	4.30	4.25	4.50
4	Feldspar-Plagioclase	3.00	3.25	3.50	4.20	4.00	4.00
5	Quartz-Plagioclase	3.00	3.10	3.20	3.50	3.75	3.50
6	Mica-Mica	3.00	3.00	3.00	2.90	3.25	3.00
7	Mica-Quartz	3.00	2.90	2.80	2.50	3.00	2.50
8	Feldspar-Quartz	3.00	2.80	2.60	2.10	2.00	2.00
9	Mica-Feldspar	3.00	2.70	2.40	1.70	1.25	1.50
10	Mica-Plagioclase	3.00	2.50	2.00	1.50	1.00	0.50

Table 4. List of input values for dilation angle. Each column corresponds to a different set of parameters, where the "Range" (minimum value subtracted from maximum value) indicates the level of heterogeneity. 0 range is the base case listed in Table 1.

	Range	**0**	**1**	**2**	**3**	**4**	**5**	**6**	**7**	**8**	**9**
	Minimum	5.00	4.50	4.00	3.50	3.00	2.50	2.00	1.50	1.00	0.50
Ranking	Maximum	5.00	5.50	6.00	6.50	7.00	7.50	8.00	8.50	9.00	9.50
1	Quartz-Quartz	5.00	5.50	6.00	6.50	7.00	7.50	8.00	8.50	9.00	9.50
2	Plagioclase-Plagioclase	5.00	5.45	5.75	6.00	6.25	7.00	7.50	8.25	8.50	9.00
3	Feldspar-Feldspar	5.00	5.35	5.75	6.00	6.25	6.75	7.00	7.25	8.00	8.50
4	Feldspar-Plagioclase	5.00	5.25	5.50	5.75	6.00	6.25	6.25	6.75	7.25	7.50
5	Quartz-Plagioclase	5.00	5.10	5.25	5.25	6.00	5.75	6.25	6.50	6.50	6.25
6	Mica-Mica	5.00	5.00	5.00	5.00	5.25	5.00	5.50	5.00	5.00	5.50
7	Mica-Quartz	5.00	4.90	4.75	5.00	4.25	4.50	4.50	4.00	4.00	3.50
8	Feldspar-Quartz	5.00	4.80	4.50	4.50	4.25	4.00	3.50	3.00	3.00	2.25
9	Mica-Feldspar	5.00	4.70	4.50	4.25	3.50	3.50	2.50	2.75	2.00	1.50
10	Mica-Plagioclase	5.00	4.50	4.00	3.50	3.00	2.50	2.00	1.50	1.00	0.50

3. MODEL ANALYSIS

During simulations, average axial stress, average axial strain, average lateral strain, and the proportion of cracks failing in tension and shear were tracked to monitor macroscopic properties of the stress-strain behavior of the BBM. These macroscopic properties are Young's Modulus, Poisson's Ratio, UCS and peak strength, and CI and CD. The methods for determining each of these properties are discussed subsequently.

3.1. Young's Modulus and Poisson's Ratio

Macroscopic Young's Modulus and Poisson's Ratio are elastic parameters, and are determined using the linear elastic portion of the axial stress, axial strain, and lateral strain data. Young's Modulus is equivalent to the slope of the axial stress-axial strain curve within this linear elastic region, and Poisson's Ratio is equivalent to the slope of the lateral strain-axial strain curve within the linear elastic region.

3.2. UCS and Peak Strength

The overall strength of the BBM is referred to as the "UCS" when there is zero confining pressure, and the "peak strength" when under 12 MPa of confining pressure. Strength is assessed by identifying the largest stress achieved by the BBM during the simulation.

3.3. Crack Initiation (CI)

Crack Initiation, commonly referred to as CI, is defined as the stress at the onset of inelastic straining in the lateral direction, which is equivalent to the point of nonlinearity

in the axial stress-lateral strain curve, as well as the point of reversal in crack volumetric strain (Diederichs and Martin, 2010). Two common methods for determining CI in BBMs is to (1) find the point of non-linearity in the axial strain-lateral strain curve and (2) find the deviation from horizontality in the Inverse Tangent Lateral Stiffness (ITLS) curve (Ghazvinian et al., 2012; Clark et al., 2019; Sinha and Walton, 2020).

Micromechanically (i.e., at the grain scale), CI is equivalent to the point of acceleration of the formation of tensile cracks within the specimen. So, CI can additionally be determined from a tensile crack curve by evaluating the intersection of the second and third linear regions (Sinha and Walton, 2020).

These three methods for CI determination for BBMs are illustrated in Figure 1. The average value of CI determined via the three methods was used as CI in this study.

3.4. Crack Damage (CD)

Crack Damage, commonly referred to as CD, is defined as the stress at the onset of inelastic straining in the axial direction, which is equivalent to the point of nonlinearity in the axial stress-axial strain curve (Diederichs and Martin, 2010). While it has previously been suggested that this point is coincident with the point of volumetric strain reversal, studies have shown that the volumetric strain reversal point does not coincide with CD under confined conditions (Diederichs and Martin, 2010; Sinha et al., 2020). Thus, for laboratory specimens, CD is determined primarily using two methods: (1) the point of non-linearity in the axial stress-axial strain curve and (2) the point of deviation from horizontality in the instantaneous Young's Modulus curve. The volumetric strain reversal point method can be used for unconfined cases in non-porous rocks, such as Blanco Mera granite. These three methods are illustrated in Figure 2.

Micromechanically (i.e., at the grain scale), CD is equivalent to the point of acceleration of the formation of shear cracks within the specimen. Figure 3 displays a fourth process for determining CD in BBMs by finding the intersection of the second and third linear regions in the shear crack curve (Sinha and Walton, 2020). This method was used, in conjunction with the three methods discussed previously, to determine CD for the BBM simulations. An average value of the applicable methods was calculated to assign CD to each simulation.

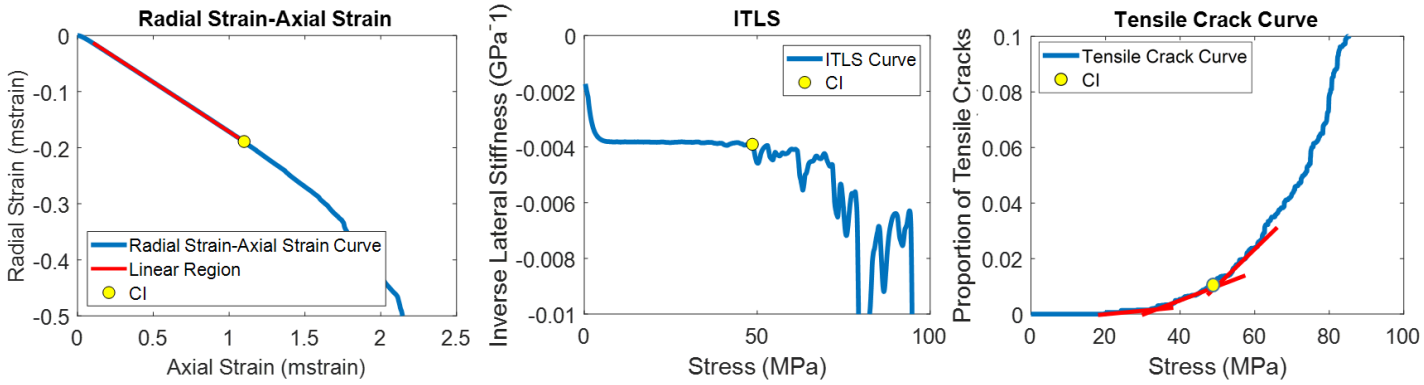

Figure 1. Determination of the Crack Initiation (CI) parameter for the BBM using the lateral (radial) strain-axial strain plot (left), the Inverse Tangent Lateral Stiffness (center), and the tensile crack (right) methods. All methods show the same CI of 50 MPa. Note: the "Linear Region" in the left hand figure does not correspond to the elastic region.

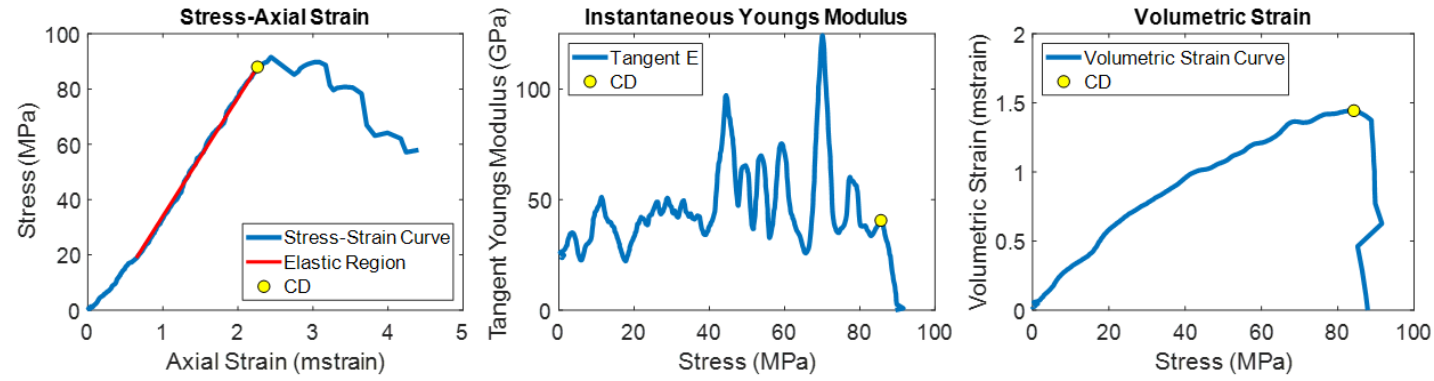

Figure 2. Three methods for determining CD of a laboratory specimen under no confining pressure (UCS). Left is the point of non-linearity in the axial stress-axial strain curve, center is the point of non-linearity of instantaneous Young's Modulus (ignoring local peaks of troughs), and right is the volumetric strain reversal point. Only left and center methods should be used for specimens tested under confined conditions. For this UCS specimen, all methods coincide to show a CD of 85 MPa.

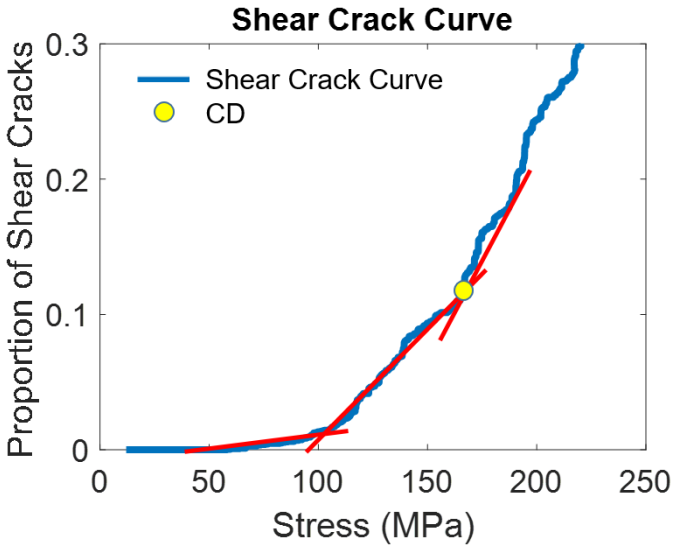

Figure 3. A fourth method for determining CD under any confinement level. CD is the intersection between the second and third linear portions of the crack curve (shown in red).

4. RESULTS

For each model set, the macroscopic behavior of the BBM under unconfined conditions and confined conditions with 12 MPa of confinement were analyzed, as discussed in Section 3. Results for each macroscopic property were normalized to the average value for that input parameter set, and the data was plotted as a function of the heterogeneity factor (HF) (Eq. 1) or range (Tables 3 and 4). An example of this normalization process is shown in Figure 4.

Visual assessment confirmed that a linear model could appropriately fit the trends of the data. Thus, a linear regression line was fit to the normalized data for each case, and a linear trend was considered for analysis if it had an R^2 value of greater than 0.5. The trends that satisfy this requirement are summarized in Table 5 (the linear regression results of an input parameter's effect on a macroscopic BBM property were not included in Table 5 if the R^2 value was less than 0.5).

To emphasize the most notable trends, those corresponding to R^2 values greater than 0.65 and normalized trend slope with absolute magnitude greater than 5% are highlighted in yellow in Table 5. Note that a trend slope magnitude of 5% indicates that when the heterogeneity of the given input parameter is doubled, the output property being considered changes by 5%. Therefore, trend slope magnitudes lower than 5% signify a negligible change in the BBM's macroscopic property value as a function of heterogeneity of the given input parameter. Plots for each highlighted data set are included as Figures 5 and 6.

In examining the results shown in Table 5, in can be seen that Young's Modulus, Poisson's Ratio, confined strength, unconfined CI, and the ratio of CI to strength

Table 5. Summary of results (with R^2 of at least 0.5) of the macroscopic properties of the BBM that were affected by the heterogeneity of an input parameter. Normalized percent trend and R^2 values are calculated via linear regression (Figure 4). A negative percent change indicates a decrease in the property's value from the base BBM (Table 1). Highlighted cells correspond to those with an R^2 of at least 0.65 and a normalized percent trend of at least 5% (absolute value).

Macroscopic BBM Property	Input Parameter	Normalized Trend	R^2
Young's Modulus	--	--	--
Poisson's Ratio	joint normal stiffness	-1.2%	0.54
	residual friction angle	+0.3%	0.54
UCS	joint shear stiffness	-8.7%	0.62
	peak cohesion	-13.2%	0.85
	dilation angle	-0.2%	0.61
Strength (12 MPa)	friction angle	-4.2%	0.83
CI (UCS)	--	--	--
CI (12 MPa)	joint normal stiffness	+6.4%	0.65
CI/UCS	dilation angle	-0.2%	0.64
CI/Strength (12 MPa)	joint normal stiffness	+13.4%	0.58
CD (UCS)	joint normal stiffness	-9.3%	0.57
	peak cohesion	-41.2%	0.94
	peak friction angle	-6.1%	0.65
CD (12 MPa)	joint normal stiffness	-11.6%	0.69
	peak cohesion	-28.8%	0.89
	peak friction angle	-7.8%	0.79
	residual friction angle	-1.5%	0.77
CD/UCS	peak cohesion	-28.9%	0.87
	dilation angle	-0.2%	0.56
CD/Strength (12 MPa)	joint shear stiffness	-8.6%	0.59
	peak cohesion	-29.1%	0.83

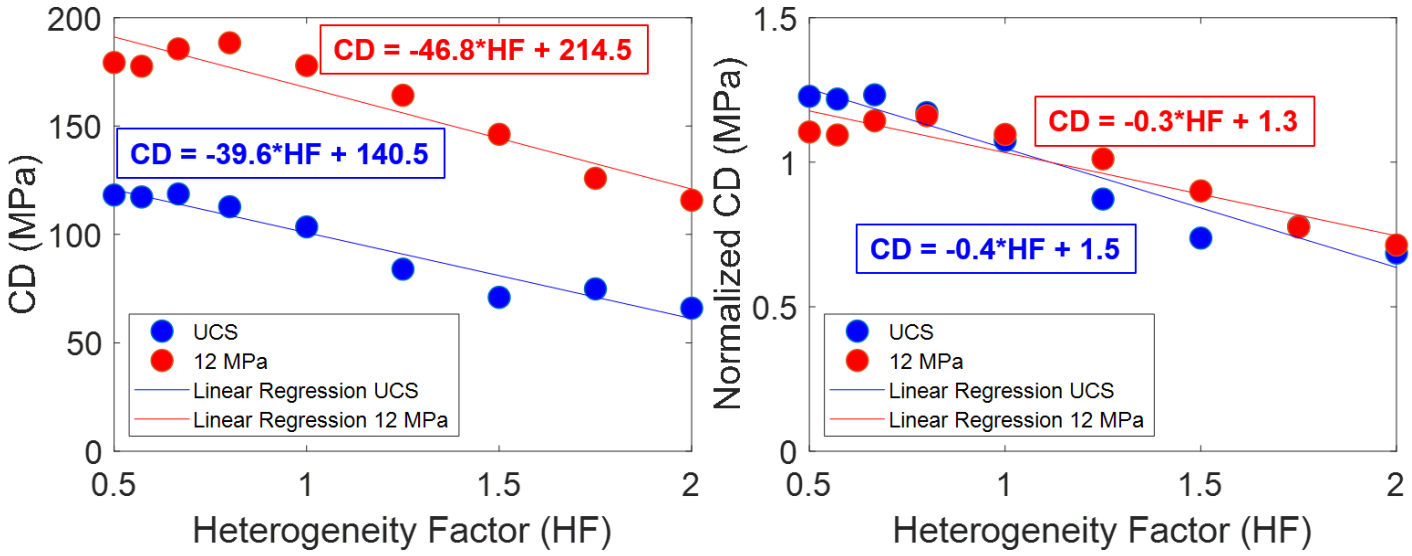

Figure 4. Example of normalization of data. The raw data (left) for the CD of the BBM, as a function of the heterogeneity factor (HF) of contact peak cohesion, was normalized by dividing each raw data point by the average CD value for all HFs tested in the set. The average CD for the UCS tests was 96.3 MPa and the average CD for the confined tests with 12 MPa of confinement was 162.3 MPa. The normalized data is plotted on the right hand figure. Linear regression lines of both raw data and normalized data are included with their equations, for both confinement cases.

were not significantly affected by changing the heterogeneity of any contact input parameter.

Additionally, the heterogeneity of contact joint shear stiffness, peak tensile strength, residual friction angle, and dilation angle had negligible effects on the BBM's behavior, as defined by the criteria discussed above.

The heterogeneity of contact peak cohesion, peak friction angle, and joint normal stiffness were found to have an effect on the macroscopic behavior of the BBM, which will be discussed in subsequent sections.

Although the entirety of data analysis has been done using linear regression, a non-linear trend was noted in the majority of results highlighted in Table 5. This trend can be observed in both the raw data plot and the normalized data plot of Figure 4. Decreasing the heterogeneity from the base case (HF = 1) to HF values less than 1 appears to have a smaller effect on the macroscopic BBM property than increasing the heterogeneity from the base case to HF values greater than 1. This "kink" in the linear trend seems to correspond to approximately an HF of 1, which is the base (i.e. calibrated) input parameter set.

4.1. Peak Cohesion

The most notable finding of this sensitivity analysis is that heterogeneity of contact peak cohesion has a large impact on CD values, both under unconfined and confined conditions. According to the linear regression models, increasing the HF from 1 to 2 decreased the BBM's normalized CD by 41.2% under unconfined conditions, and by 28.8% in the case with 12 MPa of confinement (see Figure 6a). This same trend is observed when analyzing the normalized ratio of CD to Strength, where increasing HF from 1 to 2 decreased this ratio by 28.9% and 29.1% for the unconfined and confined cases, respectively (see Figure 6b).

The heterogeneity of peak cohesion was also found to affect the UCS of the BBM. According to the linear regression models, increasing HF of peak cohesion from 1 to 2 decreased the BBM's normalized UCS by 13.2% (see Figure 5). Although the heterogeneity of contact peak cohesion has a non-negligible effect on the BBM's UCS, it has a much larger influence on the BBM's CD.

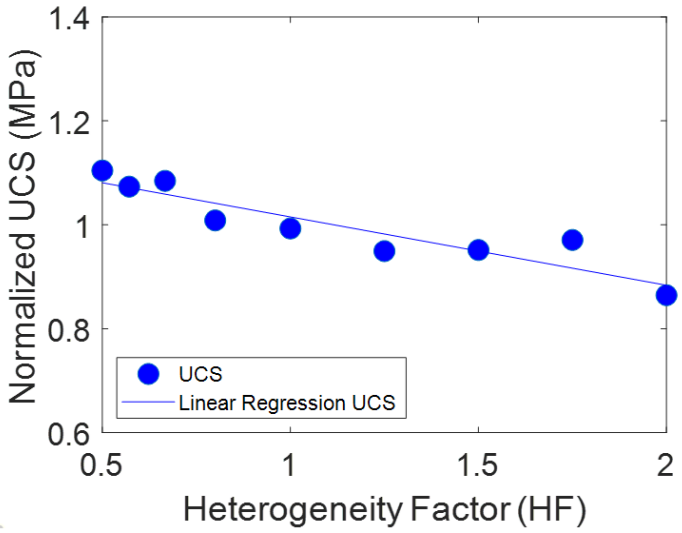

Figure 5. Trend in the UCS of the BBM as a function of the variation of the heterogeneity of peak cohesion. Data was normalized by dividing each raw data point by the average UCS value for all HFs tested in the set. The linear regression line has the percent trend and R^2 values listed in Table 5.

Peak cohesion has previously been found to have a strong effect on both the UCS and CD of BBMs, where a higher average value of contact peak cohesion results in a higher UCS (Cai and Noorani, 2015; Bahaaddini and Rahimi, 2018) and higher CD (Wang and Cai, 2019), under all confinements. Since this sensitivity analysis has found that increasing the heterogeneity of contact peak cohesion decreases UCS and CD, it appears that the minimum value assigned to contact peak cohesion is dominating the macroscopic behavior of the BBM.

4.2. Joint Normal Stiffness (jkn)

Increasing the HF of joint normal stiffness (jkn) from 1 to 2 was found to increase normalized confined CI (with 12 MPa of confinement) by 6.4% according to the linear regression model (see Figure 6c). This indicates, similarly to the case of contact cohesion discussed in Section 4.1, that the lowest jkn value is the primary control on the macroscopic behavior of the BBM. Lower stiffness requires more deformation to reach the stress level that induces contact failure, so initial failure of the weaker contacts is delayed in the higher heterogeneity cases. Note that in the case of this BBM, the 5 weakest contact types (see Tables 3 and 4 for ranking) account for 58% of the contacts in the BBM (see Table 2). This delay in contact failure when joint stiffness input parameters have higher heterogeneity results in a delay in CI, which is controlled by tensile failure of contacts. It is unclear why this effect appears to be notable under confined conditions, but not unconfined conditions.

Increasing the HF of joint normal stiffness (jkn) from 1 to 2 was also found to decrease normalized confined CD

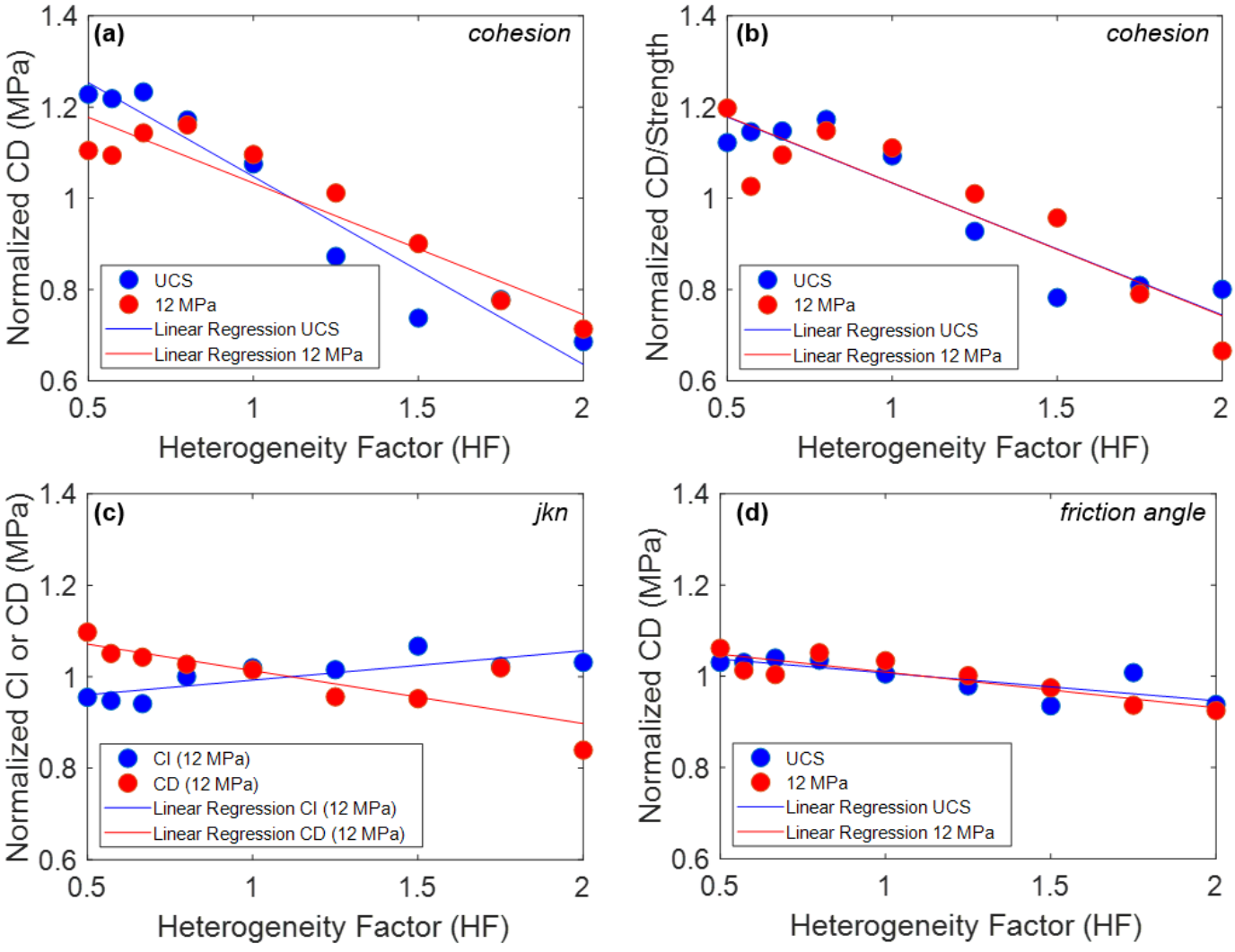

Figure 6. Non-negligible results. Normalized data is plotted as circles, which were normalized by dividing raw data points by the average value for all HFs tested in the sets. The corresponding percent trend and R^2 values of the plotted linear regression lines are listed as the highlighted cells in Table 5. The input parameter whose heterogeneity factor has been varied (the X-axis) is written in italics in the top right corner of each plot. The macroscopic property of the BBM is the Y-axis. (a) Trend in unconfined and confined CD as a function of the heterogeneity variation of peak cohesion, (b) Trend in unconfined and confined CD/Strength ratio as a function of the heterogeneity variation of peak cohesion, (c) Trend in confined CI and CD as a function of the heterogeneity variation of joint normal stiffness, (d) Trend in unconfined and confined CD as a function of the heterogeneity variation of peak friction angle.

(with 12 MPa of confinement) by 11.6%, according to the linear regression model (see Figure 6c). Micromechanically, more heterogeneity of contact normal stiffness correlates to larger differences in relative normal displacement of blocks within the BBM before contact failure occurs. This differential displacement generates local stress concentrations and contributes to contacts in certain regions failing before others. Since CD is equivalent to the point of acceleration of shear contact failure, CD occurs earlier in BBMs where these micromechanical stress concentrations are more prominent (e.g. larger joint stiffness heterogeneity).

This same micromechanical process affects unconfined CD as well, but to a lesser degree. Table 5 shows a decrease in normalized unconfined CD of 9.3% when the HF of jkn is increased from 1 to 2, according to the linear regression model. However, this trend only has an R^2 value of 0.57 (and is therefore not presented in Figure 6).

Failure of contacts, both in tension (associated with CI) and in shear (associated with CD), is influenced by stress concentrations. These stress concentrations can be created by both jkn and jks heterogeneity. So although CD is associated with shear failure of contacts, both jkn and jks heterogeneity create stress concentrations that fail contacts, which affects the CD of the BBM. It is unclear why this trend is not also observed for CI.

These micromechanical processes apply to heterogeneity in joint shear stiffness (jks), as well. However, since pre-peak intact brittle rock damage processes are predominantly tensile in nature, micromechanical stress concentrations are largely associated with jkn heterogeneity. Additionally, since jks values were lower than jkn values in the base BBM (see Table 1), contacts displace less in shear than in tension given the same stress level. This causes less intense local stress concentrations due to jks heterogeneity.

4.3. Peak Friction Angle

The heterogeneity of contact peak friction angle was found to have a minor effect on the normalized CD of the BBM, with decreases of 6.1% and 7.8% per unit increase in HF in the linear regression models under 0 MPa and 12 MPa of confinement, respectively (see Figure 6d). The average value of peak friction angle has previously been found to have an effect on the CD of a BBM, where an increase in the average contact peak friction angle results in a higher CD, under all confinements (Farahmand and Diederichs, 2015). Therefore, since increasing the heterogeneity of the input parameter values resulted in a decrease in CD, for both the UCS and Triaxial test simulations, it appears that the minimum value assigned to contact friction angle is a notable control on the macroscopic behavior of the BBM, similar to the cases discussed in Sections 4.1 and 4.2.

5. CONCLUSION

A sensitivity analysis was conducted on the heterogeneity of contact input parameters in Bonded Block Models (BBMs). An elastic block BBM of Blanco Mera granite that had been previously calibrated to laboratory data (West et al., 2020) was used as the basis for this study, which includes four different mineral (block) types and 10 distinct contact types. The input parameters for the contacts include normal and shear stiffnesses, peak cohesion, peak friction angle, peak tensile strength, residual friction angle, and dilation angle.

Each of these seven contact properties were tested separately by varying the degree of heterogeneity within contact types, while keeping the weighted average of the contact property constant for all simulations. Both a UCS test and a Triaxial test with 12MPa of confinement were simulated for each variation of the contact input parameters. Macroscopic material properties were computed from the model results including Young's Modulus, Poisson's Ratio, UCS and Peak Strengths, and Crack Initiation (CI) and Crack Damage (CD) parameters.

Young's Modulus, Poisson's Ratio, confined strength, unconfined CI, and the ratio of CI/Strength were found to be insensitive to the heterogeneity of any of the contact input parameters. Thus, these material properties are dependent only on average values for certain input parameters.

The heterogeneity of peak cohesion was found to have a major effect on the BBM's UCS and CD (unconfined and confined), as well as the ratio of CD to strength under unconfined and confined conditions. The heterogeneity of peak friction angle was found to affect CD (unconfined and confined), and the heterogeneity of joint normal stiffness was found to affect confined CI and CD.

Although the macroscopic behavior of the BBM was found to be sensitive to the heterogeneity of multiple input parameters, only the heterogeneity of peak cohesion caused a large change in the model behavior (i.e. normalized percent trends of greater than 25% in the linear regression models). So, it appears BBMs are primarily controlled by their average contact input properties, with the exception of peak cohesion, the heterogeneity of which considerably affects the model's CD.

This sensitivity analysis only applies to one BBM with one grain (i.e. block) structure. This grain structure dictates the percentage of the different contact types within the model. Since many of the notable results discussed in Section 4 depend on micromechanical processes on the grain-scale level, changing the BBM grain structure would likely change the results. The heterogeneity of certain input parameters may affect the macroscopic behavior of the BBM more or less with a

different grain structure, although such differences are not expected to be large.

6. ACKNOWLEDGEMENT

The authors would like to thank Itasca Consulting Group for providing educational licenses to UDEC, which were used to run some of the models for this study.

The research conducted for this study was partially funded by the National Institute of Occupational Health and Science (NIOSH) under Grant Number 200-2016-90154. The authors would like to extend their sincere gratitude for this financial support.

REFERENCES

1. Alejano, L. R., Arzúa, J., Bozorgzadeh, N., and Harrison, J. P. 2017. Triaxial strength and deformability of intact and increasingly jointed granite samples. *International Journal of Rock Mechanics and Mining Sciences*, *95*(May 2016), 87–103.
2. Bahaaddini, M., and Rahimi, M. 2018. Distinct element modelling of the mechanical behavior of intact rocks using Voronoi tessellation model. *International Journal of Mining and Geo-Engineering*, *52*(1), 61–68
3. Bass, J.D. 1995. Elasticity of Minerals, Glasses, and Melts. Mineral Physics & Crystallography. In *A Handbook of Physical Constant, 2*.
4. Cai, M. and Noorani, R. 2015. Simulation of dilation behavior of brittle rocks using a grain-based model. In the proceedings of *13th International Congress of Rock Mechanics, Montreal, Canada*, *6*(May), 1–12.
5. Chen, W. and Konietzky, H. 2014. Simulation of heterogeneity, creep, damage and limetime for loaded brittle rocks. *Tectonophysics*, *633*(1), 164-175.
6. Chen, W., Konietzky, H., Tan, X., and Frühwirt, T. 2016. Pre-failure damage analysis for brittle rocks under triaxial compression. *Computers and Geotechnics*, *74*, 45–55.
7. Clark, M. D., Day, J. J., and Diederichs, M. S. 2019. Assessing the geomechanical behaviours of skarn-related hydrothermal veins in intact laboratory tests. In *Proceedings of 53rd U.S. Rock Mechanics/Geomechanics Symposium*.
8. Diederichs, M. S., and Martin, C. D. 2010. Measurement of spalling parameters from laboratory testing. In *Proceedings of the European Rock Mechanics Symposium, EUROCK 2010*, 323–326.
9. Farahmand, K., and Diederichs, M. S. 2015. A calibrated synthetic rock mass (SRM) model for simulating crack growth in granitic rock considering grain scale heterogeneity of polycrystalline rock. In *Proceedings of the 49th US Rock Mechanics / Geomechanics Symposium 2015*, *1*(i), 9–22.
10. Ghazvinian, E., Perras, M., Diederichs, M., and Labrie, D. 2012. Formalized approaches to defining damage thresholds in brittle rock: Granite and limestone. In *Proceedings of 46th US Rock Mechanics / Geomechanics Symposium 2012*, 2, 966–974.
11. Ghazvinian, E., Diederichs, M. S., and Quey, R. 2014. 3D random Voronoi grain-based models for simulation of brittle rock damage and fabric-guided micro-fracturing. *Journal of Rock Mechanics and Geotechnical Engineering*, *6*(6), 506–521.
12. Jing, L. 2003. A review of techniques, advances and outstanding issues in numerical modelling for rock mechanics and rock engineering. *International Journal of Rock Mechanics and Mining Sciences*, *40*(3), 283–353.
13. Norouzi, S., Baghbanan, A., and Khani, A. 2013. Investigation of grain size effects on micro/macro-mechanical properties of intact rock using voronoi element - Discrete element method approach. *Particulate Science and Technology*, *31*(5), 507–514.
14. Sinha, S., Shirole, D., and Walton, G. 2020. Investigation of the Micromechanical Damage Process in a Granitic Rock Using an Inelastic Bonded Block Model (BBM). *Journal of Geophysical Research: Solid Earth*, 125(3), 1–24.
15. Sinha, S., and Walton, G. 2020. A study on Bonded Block Model (BBM) complexity for simulation of laboratory-scale stress-strain behavior in granitic rocks. *Computers and Geotechnics*, *118*, 103363.
16. Stavrou, A., and Murphy, W. 2018. Quantifying the effects of scale and heterogeneity on the confined strength of micro-defected rocks. *International Journal of Rock Mechanics and Mining Sciences*, *102*(November 2017), 131–143.
17. Walton, G., Alejano, L. R., Arzúa, J., and Markley, T. 2018. Crack Damage Parameters and Dilatancy of Artificially Jointed Granite Samples Under Triaxial Compression. *Rock Mechanics and Rock Engineering*, *51*(6), 1637–1656.
18. Wang, X., and Cai, M. 2019. A comprehensive parametric study of grain-based models for rock failure process simulation. *International Journal of Rock Mechanics and Mining Sciences*, *115*, 60–76.
19. West, I., Walton, G., and Sinha, S. 2020. Simulating the Behavior of Compressively Loaded Blanco Mera Granite Using Bonded Block Models. In *Proceedings of the 54th US Rock Mechanics/Geomechanics Symposium.*